Arnold's cat map dynamics in a system of coupled nonautonomous van der Pol oscillators

Olga B. Isaeva, Alexey Yu. Jalnine, and Sergey P. Kuznetsov
Institute of Radio-Engineering and Electronics of RAS, Saratov Branch, Zelenaya 38, Saratov 410019, Russian Federation
(Received 20 June 2006; published 9 October 2006)

An example of a flow system is presented with an attractor concentrated mostly at a surface of a two-dimensional torus, the dynamics on which is governed by the Arnold cat map. The system is composed of four coupled nonautonomous van der Pol oscillators. Three of them have equal characteristic frequencies, and in the other one the frequency is twice as large. The parameters controlling excitation of the two pairs of oscillators are forced to undergo a slow counterphase periodic modulation in time. At the end of the active stage for one pair of the oscillators, the excitation is passed to another pair, than back, and so on. In terms of a stroboscopic Poincaré section, the respective eight-dimensional (8D) mapping, due to strong phase volume compression, reduces approximately to a 2D map for the phases of one pair of the oscillators that corresponds approximately to the Arnold cat map. The largest two Lyapunov exponents (one positive and one negative) are close to those predicted with the cat map model. Estimates for the fractal dimension of the attractor of the Poincaré map are close to 2.

DOI: 10.1103/PhysRevE.74.046207 PACS number(s): 05.45.−a

Mathematical studies in nonlinear dynamics and chaos theory have advanced many concepts and models of fundamental significance. However, in some cases the relation of them to realistic physical systems is not understood well.

In mathematically oriented textbooks and reviews, much attention is devoted to Anosov hyperbolic automorphisms of a torus [1–6]. The most popular example is an iterative map,

$$p_{n+1} = p_n + q_n \pmod 1,$$

$$q_{n+1} = p_n + 2q_n \pmod 1. \tag{1}$$

In the literature, it is known as Arnold's cat map because of the use of a picture of a cat's face in explanations of the action of this map in lectures and books of Arnold. For graphical representation it is convenient to regard the phase-space of the model as a unit square on a plane with the opposite pairs of sides identified. The map (1) is a conservative system: any domain in the (p,q) plane (say, that cat face) conserves its area under iteration.

It is known that the map (1) demonstrates chaotic dynamics in the sense of the hyperbolic theory of Smale and Anosov [1–8], with such attributes as the existence of continuous invariant measure, a possibility of description in terms of Markov partition and symbolic dynamics, positive topological and metric entropies, etc. Two Lyapunov exponents are expressed via eigenvalues of the matrix associated with the map, namely,

$$\Lambda_1 = \ln(3+\sqrt{5})/2 = 0.9624,$$

$$\Lambda_2 = -\ln(3+\sqrt{5})/2 = -0.9624. \tag{2}$$

The larger exponent is positive; that reflects the presence of exponential sensitivity with respect to initial conditions, which is one of the principal features of chaos.

In this paper we propose an example of a nonautonomous flow system, in which a set of two phase variables observed stroboscopically follows the Arnold cat map to a good approximation. The main idea is adopted from a recent work of one of the authors [9]. The system is composed of two pairs of coupled nonautonomous self-oscillators. Due to slow modulation of the parameters responsible for the self-excitation, these two pairs of oscillators become active turn by turn, and because of the presence of appropriately introduced coupling they pass the excitation from one to the other.

To start, let us remark that because of the matrix relation,

$$\begin{pmatrix} 1 & 1 \\ 1 & 2 \end{pmatrix} = \begin{pmatrix} 0 & 1 \\ 1 & 1 \end{pmatrix} \begin{pmatrix} 0 & 1 \\ 1 & 1 \end{pmatrix}, \tag{3}$$

the Arnold cat map may be represented as a twofold composition of a simpler map:

$$p_{n+1} = q_n \pmod 1,$$

$$q_{n+1} = p_n + q_n \pmod 1. \tag{4}$$

To implement the corresponding dynamics in a physical system, we consider a set of four coupled nonautonomous van der Pol oscillators:

$$\ddot{x} - [A\cos(2\pi t/T) - x^2]\dot{x} + \omega_0^2 x = \varepsilon z \cos\omega_0 t,$$

$$\ddot{y} - [A\cos(2\pi t/T) - y^2]\dot{y} + \omega_0^2 y = \varepsilon w,$$

$$\ddot{z} - [-A\cos(2\pi t/T) - z^2]\dot{z} + 4\omega_0^2 z = \varepsilon xy,$$

$$\ddot{w} - [-A\cos(2\pi t/T) - w^2]\dot{w} + \omega_0^2 w = \varepsilon x. \tag{5}$$

Three of them (x, y, and w) have equal basic frequencies ω_0, and the remaining one (z) has a frequency $2\omega_0$. The control parameter responsible for the Andronov-Hopf bifurcation in autonomous partial systems is forced to oscillate slowly with some period T, much larger than $2\pi/\omega_0$. For one half period the first pair of oscillators (x,y) is active, i.e., is above the self-oscillation threshold, while the second pair (z,w) is passive, i.e., is below the self-oscillation threshold. For the other half period the situation is the opposite. The oscillators x and

y affect the oscillator z via the term represented by the product xy, which contains a component close to the doubled basic frequency. It serves as a priming for the oscillator z as it becomes active due to the parameter variation. At the same time, the oscillator w accepts excitation from the oscillator x. Then, as the active stage for the second pair of oscillators comes to the end, the excitation returns to the first pair. Now, the oscillator z affects the oscillator x via the coupling term represented as the product of z and the auxiliary signal of frequency ω_0, and the oscillator y accepts excitation from the oscillator w.

We assume that the period of the slow parameter modulation contains an integer number of periods of the auxiliary signal $N_0=\omega_0 T/2\pi$, so the external driving is periodic.

Let us derive relations in rough approximation for the phases of the oscillators in the course of the process. Suppose that the first and the second oscillators on an active stage of the process have some initial phases φ_x and φ_y:

$$x \propto \cos(\omega_0 t + \varphi_x), \quad y \propto \cos(\omega_0 t + \varphi_y). \tag{6}$$

The coupling term in the third equation contains a product

$$xy \propto \cos(\omega_0 t + \varphi_x)\cos(\omega_0 t + \varphi_y) = (1/2)[\cos(\varphi_x - \varphi_y) + \cos(2\omega_0 t + \varphi_x + \varphi_y)]. \tag{7}$$

The last component in the expression is of frequency close to that of the oscillator z and excites it effectively. So, on the stage of activity, the third oscillator inherits the phase $\varphi_z \approx \varphi_x + \varphi_y + \text{const}$, while the fourth oscillator simply accepts the phase of the first one: $\varphi_w \approx \varphi_x + \text{const}$. At the beginning of the next stage of activity for the oscillators x and y the coupling term in the first equation

$$z\cos\omega_0 t \propto (1/2)[\cos(3\omega_0 t + \varphi_x + \varphi_y) + \cos(\omega_0 t + \varphi_x + \varphi_y)] \tag{8}$$

excites the oscillator x, and it acquires the phase $\varphi_x' \approx \varphi_z + \text{const} \approx \varphi_x + \varphi_y + \text{const}$. The oscillator y inherits the phase from w: $\varphi_y' \approx \varphi_w + \text{const} \approx \varphi_x + \text{const}$. So, we come to an approximate mapping for the phases,

$$\varphi_x' = \varphi_x + \varphi_y + \text{const}, \quad \varphi_y' = \varphi_x + \text{const}. \tag{9}$$

With normalization $q=\varphi_x/2\pi$ and $p=\varphi_y/2\pi$ we obtain exactly the map (4), up to some additive constants. (By an appropriate shift of the origin they may be removed.) Hence the stroboscopic dynamics observed with the basic time interval $2T$ for the phases of the oscillators (x,y) will follow the Arnold cat map, at least in the approximation we have considered. One of the consequences is that the dynamics of the phases will manifest chaos with strong statistical properties.

To support this conclusion, let us turn to direct numerical computations for the set of nonautonomous differential equations (5). Figure 1 shows plots for the variables x, y, z, and w versus time in the system (5), at parameter values

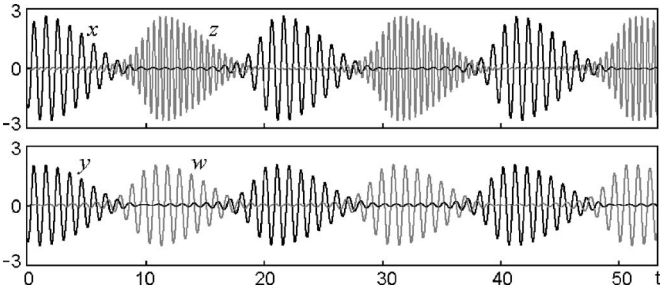

FIG. 1. Time dependence for the dynamical variables of the system (5) at $\omega_0=2\pi$, $T=20$, $A=2$, $\varepsilon=0.4$.

$$\omega_0 = 2\pi, \quad N_0 = T = 20, \quad A = 2, \quad \varepsilon = 0.4. \tag{10}$$

It operates in a chaotic regime in correspondence with the mechanism discussed. The chaotic nature of the dynamics reveals itself in a random walk of waveforms for the oscillating variables with respect to the envelope.

To demonstrate the correspondence of the dynamics to the Arnold cat map, we implement the following procedure. In the course of numerical integration of Eqs. (5) we determine the phases for the first and the second oscillators in the middle of an excitation stage as [16]

$$\varphi_x = \arg(x - i\dot{x}/\omega_0), \quad \varphi_y = \arg(y - i\dot{y}/\omega_0). \tag{11}$$

If the point $(q,p)=(\varphi_x/2\pi, \varphi_y/2\pi)$ hits the area of the cat face drawn in the unit square, we mark the dot on the diagram and the dots for the images after the time intervals $2T$ and $4T$ on two subsequent plots, respectively. By accumulation of a great number of dots, we can observe the cat face on the first picture, and the images corresponding to one and two iterations of the Arnold map on the second and the third ones [see Fig. 2(a)].

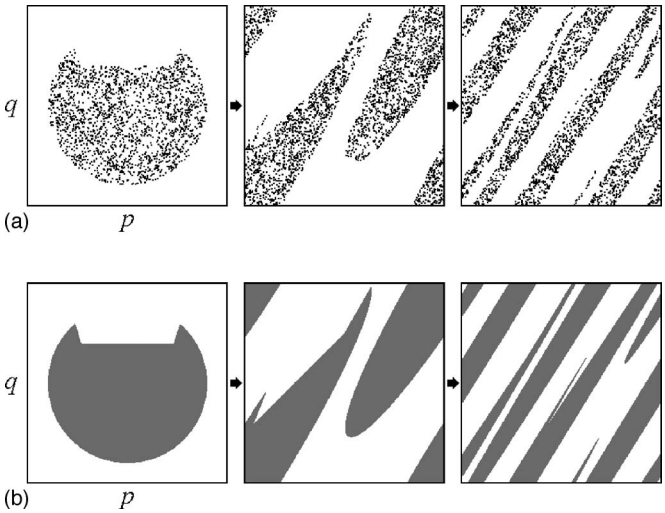

FIG. 2. Transformation of the area in a form of cat face in a plane of phase variables in a system of van der Pol oscillators (5) after time intervals $2T$ and $4T$ (a) and analogous pictures obtained from the map (12) (b).

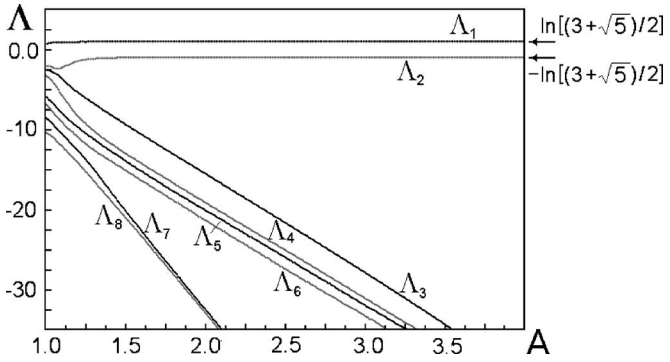

FIG. 3. Lyapunov exponents for the system (5) vs the amplitude of parameter modulation at $\omega_0=2\pi$, $T=20$, $\varepsilon=0.4$.

The pictures may be compared with those obtained directly from iterations of the Arnold cat map. To achieve an accurate correspondence, we have to account for the additional constant terms in the equations, which appear in the course of the transfer of excitations from oscillators to their partners. With these constants empirically selected [for the particular case under consideration, see Eq. (10)] the map reads

$$p_{n+1} = p_n + q_n + 0.07 \quad (\mathrm{mod}1),$$

$$q_{n+1} = p_n + 2q_n - 0.38 \quad (\mathrm{mod}1). \tag{12}$$

The plots illustrating evolution of the cat face in accordance with this map are shown in Fig. 2(b). Observe a nice correspondence between the phase dynamics in the system of nonautonomous van der Pol oscillators and in the modified Arnold cat map (12).

For a more accurate discrete-time description, we have to turn to the Poincaré map [4–6]. Let us have a certain state of the system at $t_n=2nT$, the vector $\mathbf{x}_n=\{x,\dot{x}/\omega_0, y,\dot{y}/\omega_0,z,\dot{z}/2\omega_0,w,\dot{w}/\omega_0\}$. From solution of the differential equations (5) with the initial state $\mathbf{x}_n$, we get after time interval $2T$ a new vector $\mathbf{x}_{n+1}$ determined uniquely by the vector $\mathbf{x}_n$. Therefore we introduce a function that maps the eight-dimensional space $\{x,\dot{x}/\omega_0,y,\dot{y}/\omega_0,z,\dot{z}/2\omega_0,w,\dot{w}/\omega_0\}$ into itself:

$$\mathbf{x}_{n+1} = \mathbf{T}(\mathbf{x}_n). \tag{13}$$

Geometrically, in the nine-dimensional extended phase space of our nonautonomous system $\{x,\dot{x}/\omega_0,y,\dot{y}/\omega_0,z, \dot{z}/2\omega_0,w,\dot{w}/\omega_0,t\}$ we have a cross section of the flow by the eight-dimensional hyperplanes $t=t_n=2nT$. Because of the periodicity of the phase space in t, these hyperplanes may be identified, and we speak of the mapping of the eight-dimensional hyperplane $\{x,\dot{x}/\omega_0,y,\dot{y}/\omega_0,z,\dot{z}/2\omega_0,w,\dot{w}/\omega_0\}$ into itself. The Poincaré map appears due to evolution determined by differential equations with smooth and bounded right-hand parts in a finite domain of eight variables. In accordance with theorems of existence, uniqueness, continuity, and differentiability of solutions of differential equations, the map $\mathbf{T}$ is a diffeomorphism in $\mathbb{R}^8$, a one-to-one differentiable map of class $\mathbb{C}^\infty$ [10].

To have a quantitative indicator of chaos we turn to the Lyapunov exponents. In computations, the Lyapunov exponents are evaluated for the Poincaré map with the help of the appropriately adapted algorithm of Benettin [11]. It is based on simultaneous solution of Eqs. (5) together with a collection of eight exemplars of the linearized equations for perturbations:

$$\ddot{\tilde{x}} + 2x\dot{x}\tilde{x} - [A\cos(2\pi t/T) - x^2]\dot{\tilde{x}} + \omega_0^2\tilde{x} = \varepsilon\tilde{z}\cos\omega_0 t,$$

$$\ddot{\tilde{y}} + 2y\dot{y}\tilde{y} - [A\cos(2\pi t/T) - y^2]\dot{\tilde{y}} + \omega_0^2\tilde{y} = \varepsilon\tilde{w},$$

$$\ddot{\tilde{z}} + 2z\dot{z}\tilde{z} - [-A\cos(2\pi t/T) - z^2]\dot{\tilde{z}} + 4\omega_0^2\tilde{z} = \varepsilon(\tilde{x}y + x\tilde{y}),$$

$$\ddot{\tilde{w}} + 2w\dot{w}\tilde{w} - [-A\cos(2\pi t/T) - w^2]\dot{\tilde{w}} + \omega_0^2\tilde{w} = \varepsilon\tilde{x}. \tag{14}$$

In the course of the solution, at the time instants $t=2nT$ ($n=1,2,\ldots$) the Gram-Schmidt orthogonalization and normalization are performed for eight vectors $\{\tilde{x},\dot{\tilde{x}}/\omega_0,\tilde{y},\dot{\tilde{y}}/\omega_0,\tilde{z},\dot{\tilde{z}}/2\omega_0,\tilde{w},\dot{\tilde{w}}/\omega_0\}$, and the mean rates of growth or decrease of the accumulated sums of logarithms of the norms (after the orthogonalization but before the normalization) are estimated [11]. As found, the Lyapunov exponents for the attractor at the parameters (10) are [17]

$$\Lambda_1 = 0.962, \quad \Lambda_2 = -0.970,$$

$$\Lambda_3 = -15.525, \quad \Lambda_4 = -19.074,$$

$$\Lambda_5 = -20.053, \quad \Lambda_6 = -21.315,$$

$$\Lambda_7 = -32.444, \quad \Lambda_8 = -32.898. \tag{15}$$

In Fig. 3 we show a plot for all eight Lyapunov exponents of the system of coupled nonautonomous van der Pol oscillators versus the amplitude A of slow modulation at fixed other parameters. As seen, the largest two exponents remain almost constant in a wide interval of the parameter variation and are close to the values characteristic to the Arnold cat map [see Eq. (2)]. The other exponents are large negative. They correspond to strong compression of the phase volume along six of eight dimensions of the phase space of the Poincaré map.

Qualitatively similar dynamical behavior is observed at other integer period ratios N_0, e.g., $N_0=6$. Figure 4 shows portraits of the attractor at

$$\omega_0 = 2\pi, \quad T = 6, \quad A = 6.5, \quad \varepsilon = 0.4. \tag{16}$$

The panel (a) represents a projection of the attractor from the nine-dimensional (9D) extended phase-space on the plane of variables of the first oscillator $(x,\dot{x})$. The attractor is shown in gray scales (the darkness reflects a relative duration of residence of the orbit inside a given pixel). Black dots relate to the Poincaré cross section, i.e., to the instants $t_n=2nT$. Panel (b) shows the attractor in the Poincaré cross section on the plane $(x,\dot{x})$. As expected, it looks like a projection of a two-dimensional torus. For this attractor in the Poincaré map the Lyapunov exponents are

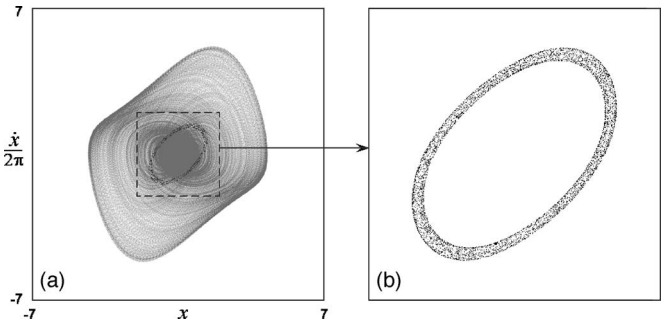

FIG. 4. Portraits of attractor at $\omega_0=2\pi$, $T=6$, $A=6.5$, $\varepsilon=0.4$: projection of the attractor from the 9D extended phase space on the plane of variables $(x,\dot{x})$ (a) and the Poincaré cross section corresponding to the instants $t_n=2nT$ that looks like a projection of 2D torus (b).

$$\Lambda_1 = 0.961, \quad \Lambda_2 = -1.021,$$

$$\Lambda_3 = -11.256, \quad \Lambda_4 = -12.908,$$

$$\Lambda_5 = -13.794, \quad \Lambda_6 = -15.886,$$

$$\Lambda_7 = -23.663, \quad \Lambda_8 = -24.464. \tag{17}$$

As found, now the linear toral map is not so good for the approximate description; it is more appropriate to use the Anosov map with added nonlinear terms:

$$p_{n+1} = p_n + q_n + f_1(p_n,q_n) \quad (\text{mod}1),$$

$$q_{n+1} = p_n + 2q_n + f_2(p_n,q_n) \quad (\text{mod}1), \tag{18}$$

where $f_1(p,q)$ and $f_2(p,q)$ are some smooth functions of period 1 in respect to both arguments. To construct this more accurate model for the dynamics under consideration, we have to determine the functions. Taking the periodicity conditions into account, they may be represented as Fourier expansions over two arguments:

$$f_{1,2}(p,q) = \sum_{n=0}^{M} \sum_{m=-M}^{M} [A_{n,m}^{1,2} \cos[2\pi(np+mq)] + B_{n,m}^{1,2} \sin[2\pi(np+mq)]. \tag{19}$$

From computations we obtain the stroboscopic sequences p_n, q_n at $t_n=2nT$, and accumulate sufficiently long series $f_{1,n}=p_{n+1}-p_n-q_n$ (mod 1) and $f_{2,n}=q_{n+1}-p_n-2q_n$ (mod 1). Then, we use a least square method and estimate the coefficients $\{A_{n,m}^{1,2}, B_{n,m}^{1,2}\}$ to obtain the best approximation for $f_{1,n}$ and $f_{2,n}$ via the Fourier expansions (19) at some finite M. Figure 5 shows 3D plots of the functions expressed via Eq. (19) at $M=12$ [left column (a)] and, for comparison, the empirical functions from the computations [right column (b)].

Figure 6 illustrates distribution of invariant measure on the attractor. Panel (a) relates to the flow system (5) and presents a large number of dots plotted on a plane of phases defined by relations (11) in the stroboscopic Poincaré cross section $t_n=2nT$. Panel (b) relates to the Anosov map (18)

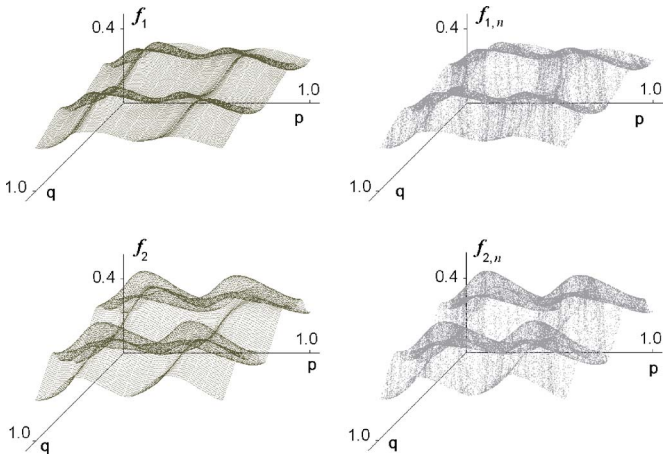

FIG. 5. (Color online) 3D plots of the nonlinear functions in the right-hand parts of the Anosov map (18) from the Fourier expansions (19) at $M=12$ (a) and empirical ones, obtained from direct computations as described in the text (b).

with the nonlinear functions expressed via the Fourier series obtained from our numerical estimates (see Fig. 5). In both cases the distribution of the density over the unit square looks similar and manifests a subtle fractal structure. Such distributions were discussed in the context of the problem of the so-called "nonstrange chaotic attractor" (NCA) [12,13,6]. In fact, the attractor in the Poincaré map of our flow system is not "nonstrange": it certainly has a transverse fractal structure in the eight-dimensional phase-space, but distribution of the invariant measure over the torus approximately representing the attractor is of the nature that has been suggested for the NCA.

To have quantitative characteristics for the fractal invariant measure on the attractor, we have estimated the correlation dimensions from the Grassberger-Procaccia algorithm [12] by processing a two-component time series composed of data for phases (11) from 10^5 iterations of the Poincaré map obtained in numerical solution of Eqs. (5) (see Fig. 7). At the present parameter values (16) we get the dimension $D_2=1.93$, notably distinct from the value 2, which would correspond to a uniform distribution of the invariant density over the surface of the 2D torus. The estimate from the

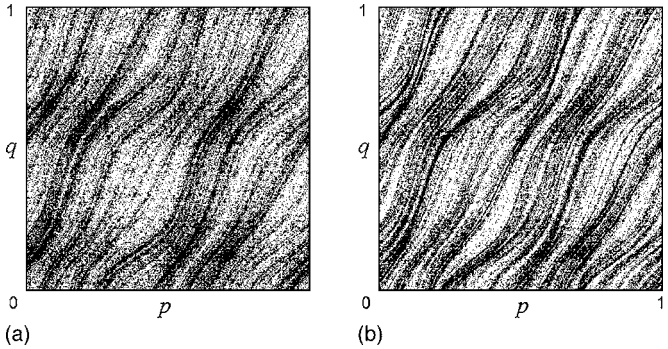

FIG. 6. Distributions of points on the attractor in projection on a plane of phases of the first pair of oscillators in Poincaré cross section obtained in computations for the system (5) at $\omega_0=2\pi$, $T=6$, $A=6.5$, $\varepsilon=0.4$ (a) and for the Anosov map (18) (b).

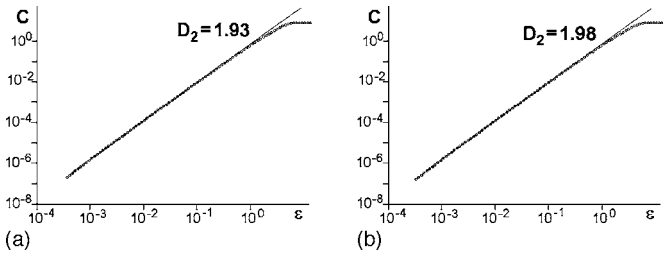

FIG. 7. Plots of the correlation integral vs the partition size obtained from processing of two-component time series of 10^5 pairs of phases (11) in the Poincaré cross section from numerical solution of Eqs. (5) at $T=6$, $A=6.5$ (a) and $T=20$, $A=2$ (b). The respective estimates for the correlation dimension correspond to a slope in the range of linear dependence.

Kaplan-Yorke formula [5] using the Lyapunov exponents (17) yields $D_L=1+\Lambda_1/|\Lambda_2|\approx 1.94$ in good agreement with the Grassberger-Procaccia result. For comparison, results for the attractor used to illustrate the cat map dynamics at the parameter set (10) are $D_2=1.98$ [see panel (b)], and $D_L=1.99$, much closer to 2.

The proposed system of four coupled nonautonomous van der Pol oscillators delivers a realistic example of dynamics approximately described by a hyperbolic map on a torus. In fact, we deal with an attractor in the eight-dimensional phase space of the Poincaré map. Due to strong phase volume compression, it reduces approximately to a two-dimensional map for the phases of one pair of the oscillators that corresponds to the Arnold cat map or to its modification with added nonlinear terms in right-hand parts of the equations. We suppose that the attractor in the Poincaré map is in fact uniformly hyperbolic and hence structurally stable, although an accurate check of this assumption (like that in Ref. [14]) seems not easy because of high dimension of the phase-space. In any case, our model obviously allows implementation, e.g., as an electronic device on a base of coupled nonautonomous self-oscillators (cf. Ref. [15]). In a similar way, many other models with dynamics of phase variables governed approximately by hyperbolic toral maps may be constructed and studied in details in numerical computations and in physical experiments.

We thank A. H. Osbaldestin for useful remarks. The work has been performed under partial support from RFBR (Grant No. 06-02-16619). O.B.I. acknowledges the support from INTAS (Grant No. 05-109-5262). A.Yu.J acknowledges the support from the Grant of the President of Russian Federation (MK-2319.2005.2).

[1] V. I. Arnold, *Geometrical Methods in the Theory of Ordinary Differential Equations* (Springer-Verlag, Berlin, 1988).
[2] V. I. Arnold and A. Avez, *Ergodic Problems of Classical Mechanics* (Benjamin, New York, 1968).
[3] R. L. Devaney, *An Introduction to Chaotic Dynamical Systems* (Addison-Wesley, New York, 1989).
[4] A. Katok and B. Hasselblatt, *Introduction to the Modern Theory of Dynamical Systems* (Cambridge University Press, Cambridge, England, 1995).
[5] S. P. Kuznetsov and I. R. Sataev, Preprint nlin. CD/0609004 (2006).
[6] V. S. Anishchenko, V. V. Astakhov, A. B. Neiman, T. E. Vadivasova, and L. Schimansky-Geier, *Nonlinear Dynamics of Chaotic and Stochastic Systems: Tutorial and Modern Development* (Springer, Berlin, Heidelberg, 2002).
[7] S. Smale, Bull. Am. Math. Soc. **73**, 747 (1967).
[8] L. A. Bunimovich *et al.*, *Dynamical Systems, Ergodic Theory and Applications*, Encyclopedia of Mathematical Sciences Vol. 100 (Springer, New York, 2000).
[9] S. P. Kuznetsov, Phys. Rev. Lett. **95**, 144101 (2005).
[10] V. I. Arnol'd, *Ordinary Differential Equations* (Springer-Verlag, Berlin, 1992).
[11] G. Benettin, L. Galgani, A. Giorgilli, and J.-M. Strelcyn, Meccanica **15**, 9 (1980).
[12] J. Farmer, E. Ott, and J. Yorke, Physica D **7**, 153 (1983).
[13] P. Grassberger and I. Procaccia, Physica D **9**, 189 (1983).
[14] S. P. Kuznetsov and I. R. Sataev (unpublished).
[15] S. P. Kuznetsov and E. P. Seleznev, JETP **102**, 355 (2006).
[16] We emphasize that the phases φ_x and φ_y cannot be determined globally, on the whole time interval T: they are attributed to a stage of excitation of the first pair of oscillators and may be used in the context of the discrete time description. Indeed, when the first pair of oscillators is below the excitation threshold, the respective amplitudes are small and the phases are not well defined.
[17] In the definition of the Lyapunov exponents we use $2T$ as the unit time to have a correspondence with the cat map model.